

Hydrodynamic stability:
Stability of shear flows

November 13, 2009

Contents

1	Introduction	5
1.1	Historical overview	5
1.2	Governing equations	6
1.2.1	Parallel flow assumption	7
1.2.2	Orr-Sommerfeld Squire system	8
1.2.3	Normal-mode assumption	9
1.2.4	Vector Modes	9
1.3	Energy equation	10
2	Inviscid results	13
2.1	Rayleigh equation	13
2.1.1	Rayleigh's inflection point criterion	13
2.1.2	Fjørtoft's criterion	14
2.2	Inviscid algebraic instability	15
2.3	Kelvin-Helmholtz instability	15
2.3.1	Instability of a vortex sheet	17
2.3.2	The piecewise mixing layer	17
3	Viscous stability	21
3.1	Squire's Transformation and Squire's Theorem	21
3.1.1	Relation between the two-dimensional and three-dimensional solutions	21
3.1.2	Damped Squire modes	22
3.1.3	Squire's theorem	22
3.2	Spectra and eigenfunctions	22
3.2.1	Continuous spectrum	22
3.2.2	Neutral stability curves	22
3.2.3	The destabilising effect of viscosity	22

Preface

These short notes are intended to help the student of the course Wave Motions and Hydrodynamic Stability (SG2221) at KTH Mechanics. They cover the second half of the course when the stability and transition of shear flows is covered. These notes are based on the book *Stability and Transition in Shear Flows* by Peter Schmid and Dan Hennigson [7]. The latter are therefore gratefully acknowledged for letting me use material from the book. I would like to stress again here that these notes are only intended as a additional material for the students attending the lectures. For further details and deeper explanations, students are encouraged to read the full book.

Stockholm, November 2007
Luca Brandt

Chapter 1

Introduction

1.1 Hystorical overview

The motion of a fluid is usually defined as *laminar* or *turbulent*. A laminar flow is an ordered, predictable and layered flow (from Latin “lamina”: layer, sheet, leaf) as opposed to the chaotic, swirly and fluctuating turbulent flow. In a laminar flow the velocity gradients and the shear stresses are smaller; consequently the drag force over the surface of a vehicle is much lower than in a turbulent flow. One of the major challenges in aircraft design is in fact to obtain a laminar flow over the wings to reduce the friction in order to save fuel. On the other hand a turbulent flow provides an excellent mixing in the flow because of the chaotic motion of the fluid particles, and it is therefore required in chemical reactors or combustion engines.

In real applications, as the velocity of the fluid or the physical dimension limiting the flow increase, a laminar motion cannot be sustained; the perturbations inevitably present within the flow are amplified and the flow evolves into a turbulent state. This phenomenon is called *transition*.

Transition and its triggering mechanisms are still today the object of many research efforts, even though the first studies on this field dates back to the end of the nineteenth century. The very first piece of work is traditionally considered the classical experiment of Osborne Reynolds in 1883 performed at the hydraulics laboratory of the Engineering Department at Manchester University. Reynolds studied the flow inside a glass tube injecting ink at the centerline of the pipe inlet. If the flow stayed laminar, he could observe a straight colored line inside the tube. When transition occurred, the straight line became irregular and the ink diffused all over the pipe section. He found that the value of a non dimensional parameter, later called Reynolds number, $Re = \frac{Ur}{\nu}$, where U is the bulk velocity, r the pipe radius and ν the kinematic viscosity, governed the passage from the laminar to the turbulent state. Reynolds stated quite clearly, however, that there is no a single *critical* value of the parameter Re , above which the flow becomes unstable and transition may occur; the whole matter is much more complicated. He also noted the sensitivity of the transition to disturbances in the flow before entering the tube.

ADD FIGURE OF REYNOLDS EXPERIMENT AND INK VISUALISATIONS

The knowledge of why, where and how a flow becomes turbulent is of great practical importance in almost all the application involving flows either internal or external. The present notes deals with instability and transition in the simplified case of shear flows, e.g. channel flows and the boundary layer over a flat plate subject to a uniform oncoming flow.

The transition process may be divided into three stages: receptivity, disturbance growth and breakdown. In the *receptivity* stage the disturbance is initiated inside the boundary layer. This is the most difficult phase of the full transition process to predict because it requires the knowledge of the ambient disturbance environment, which is stochastic in real applications. Typical sources of perturbations are free-stream or inlet turbulence, free-stream vortical disturbances, acoustic waves and surface roughness. Once a small disturbance is introduced, it may *grow* or decay according to the stability characteristics of the flow. Examining the equation for the evolution of the kinetic energy of the perturbation (Reynolds–Orr equation in section 1.3), a strong statement can be made on the non linear effects: the non linear terms redistribute energy among different frequencies and scales of the flow but have no net effect on the instantaneous growth rate of the energy. This implies that linear growth mechanisms are responsible for the energy of a disturbance of any amplitude to increase. After the perturbation has reached a finite amplitude, it often saturates and a new, more complicated, laminar flow is established. This new steady or quasi-steady state is usually unstable; this instability is referred to as “secondary”, to differentiate it from the “primary” growth mechanism responsible for the formation of the new unstable flow pattern. It is at this stage that

the final non linear *breakdown* begins. It is followed by other symmetry breaking instability and non linear generation of the multitude of scales and frequencies typical of a turbulent flow. The breakdown stage is usually more rapid and characterized by larger growth rates of the perturbation compared to the initial linear growth.

The following list highlights major developments in the history of research in the field of hydrodynamic stability. It is not intended to be a complete but rather to provide an outline for the material presented here.

- Reynolds pipe flow experiment (1883)
- Rayleigh's inflection point criterion (1887)
- Orr (1907) and Sommerfeld (1908) viscous equations
- Heisenberg (1924), Tollmien (1931), Schlichting (1933) viscous solutions
- Squire theorem (1933)
- Schubauer & Skramstad (1947), experimental verification of viscous solutions
- Gaster (1965), spatial stability theory
- Joseph (1976), Maximum Energy Growth
- 3D breakdown to turbulence (1962) and secondary instability theory (1983)
- Gilbert & Kleiser (1988), numerical simulation of transition to turbulence
- Huerre & Monkewitz (1990), absolute/convective instability
- Non-modal analysis (1992)

The first analytical work trying to explain the observed instability dates back to the end of the nineteenth century and was mainly based on the analysis of the inviscid problem, i.e. viscous effects are neglected. Most relevant here is Rayleigh's inflection point criterion stating necessary conditions for inviscid instability. Orr and Sommerfeld [5, 9] independently derived the equation for the instability of a viscous fluid and only twenty years later the first solutions were computed [10, 6]. However, it was not before 1947 that experimental verification of the developing stability theory could be provided [8]. Schubauer & Skramstad were then able to measure the so called Tollmien-Schlichting waves, the unstable waves developing in boundary layer flows. The extension to spatially evolving waves is due to Gaster (1965) who considered the evolution of waves generated at a fixed location. Before that, most of the analysis considered spatially periodic waves growing in time.

The breakdown to turbulence originating from the growth of the unstable Tollmien-Schlichting waves was documented by the experiments by Klebanoff and Tidstrom and Sargent [3] who observed the formation of three-dimensional modulation of the two-dimensional Tollmien-Schlichting waves. A theory for this so called secondary instability was proposed only later [2].

The recent development of computer power has allowed researcher to numerically simulate the full transition process and thus investigate the details of the final nonlinear stages of the transition process. The first simulation is from Kleiser & Gilbert in 1988.

In the last two decades, the concept of absolute/convective instability has been introduced. This allows to identify two distinct flow behaviors related to the nature of the instability. Further, the need of non-modal analysis for the instability of shear flows is now fully understood. This was pioneered by professors at KTH Mechanics among others.

1.2 Governing equations

Hydrodynamic stability theory is concerned with the response of a laminar flow to a disturbance of small or moderate amplitude. If the flow returns to its original laminar state one defines the flow as stable, whereas if the disturbance grows and causes the laminar flow to change into a different state, one defines the flow as unstable. Instabilities often result in turbulent fluid motion, but they may also take the flow into a different laminar, usually more complicated state. Stability theory deals with the mathematical analysis of the evolution of disturbances superposed on a laminar base flow. In many cases one assumes

the disturbances to be small so that further simplifications can be justified. In particular, a linear equation governing the evolution of disturbances is desirable. As the disturbance velocities grow above a few percent of the base flow, nonlinear effects become important and the linear equations no longer accurately predict the disturbance evolution. Although the linear equations have a limited region of validity they are important in detecting physical growth mechanisms and identifying dominant disturbance types.

The equations governing the general evolution of fluid flow are known as the Navier-Stokes equations. They describe the conservation of mass and momentum. For an incompressible fluid, using Cartesian tensor notation, the equations read

$$\frac{\partial u_i}{\partial t} = -u_j \frac{\partial u_i}{\partial x_j} - \frac{\partial p}{\partial x_i} + \frac{1}{\text{Re}} \nabla^2 u_i \quad (1.1)$$

$$\frac{\partial u_i}{\partial x_i} = 0 \quad (1.2)$$

where u_i are the velocity components, p is the pressure, and x_i are the spatial coordinates. In these equations, the convention of summation over identical indices has been assumed. For most flows presented in this text the streamwise direction will be denoted x_1 or x with velocity component u_1 or u , the normal direction is x_2 or y with corresponding velocity u_2 or v and the spanwise direction is x_3 or z with associated velocity u_3 or w .

These equations have to be supplemented with boundary and initial conditions, typically of the form

$$u_i(x_i, 0) = u_i^0(x_i) \quad (1.3)$$

$$u_i(x_i, t) = 0 \quad \text{on solid boundaries.} \quad (1.4)$$

The equations have been nondimensionalized by a velocity scale that is, for example, the centerline velocity (U_{CL}) for channel flows or the freestream velocity (U_∞) for boundary layer flows. The corresponding length scales are the channel half-height (h) or the boundary layer displacement thickness (δ_*). The Reynolds number is then given as $\text{Re} = U_{CL}h/\nu$ and $\text{Re} = U_\infty\delta_*/\nu$, respectively, with ν as the kinematic viscosity. The evolution equations for the disturbance can then be derived by considering a basic state (U_i, P) and a perturbed state ($U_i + u'_i, P + p'$), both satisfying the Navier-Stokes equations. Subtracting the equations for the basic and perturbed state and omitting the primes for the disturbance quantities, we find the following nonlinear disturbance equations

$$\begin{aligned} \frac{\partial u_i}{\partial t} &= -U_j \frac{\partial u_i}{\partial x_j} - u_j \frac{\partial U_i}{\partial x_j} - \frac{\partial p}{\partial x_i} + \frac{1}{\text{Re}} \nabla^2 u_i - u_j \frac{\partial u_i}{\partial x_j} \\ \frac{\partial u_i}{\partial x_i} &= 0 \end{aligned} \quad (1.5)$$

which constitute an initial/boundary value problem for the evolution of a disturbance $u_i^0 = u_i(t=0)$.

1.2.1 Parallel flow assumption

The shear flows we will consider are as example wakes, jets, mixing layers, boundary layers. All of them are characterised by slow variations in the streamwise coordinate, denoted x here, due to action of viscosity. These flows obey the boundary-layer (thin-layer) approximations, thus the base flow variations happen on the viscous time scale

$$t^{bf} = \frac{\delta^2}{\nu},$$

where δ is a typical thickness of the layers. The instability is acting on a fast convective time scale, $t^{in} = \frac{x}{U}$. Therefore, perturbations grow faster than the underlying flow changes and it is usually assumed for stability calculation that the base flow is not changing in the streamwise coordinate. Therefore We will consider the governing equations for infinitesimal disturbances in parallel flows. Let $U_i = U(y)\delta_{1i}$ be the parallel base flow, i.e., a flow in the x -direction that only depends on the wall-normal direction y .

Note that for channel flows, like Couette and plane Poiseuille flow, the base flow, solution of the Navier-Stokes equations, is exactly $U = U(y)$ and therefore no approximations are at work for these types of flow.

1.2.2 Orr-Sommerfeld Squire system

If the mean velocity profile $U_i = U(y)\delta_{1i}$ is introduced into the disturbance equations (1.5) and the nonlinear terms are neglected, the resulting equations can be written:

$$\frac{\partial u}{\partial t} + U \frac{\partial u}{\partial x} + vU' = -\frac{\partial p}{\partial x} + \frac{1}{\text{Re}} \nabla^2 u \quad (1.6)$$

$$\frac{\partial v}{\partial t} + U \frac{\partial v}{\partial x} = -\frac{\partial p}{\partial y} + \frac{1}{\text{Re}} \nabla^2 v \quad (1.7)$$

$$\frac{\partial w}{\partial t} + U \frac{\partial w}{\partial x} = -\frac{\partial p}{\partial z} + \frac{1}{\text{Re}} \nabla^2 w. \quad (1.8)$$

This set of equations is completed by the continuity equation

$$\frac{\partial u}{\partial x} + \frac{\partial v}{\partial y} + \frac{\partial w}{\partial z} = 0. \quad (1.9)$$

A prime (') denotes a y -derivative. Taking the divergence of the linearized momentum equations (1.6)-(1.8) and using the continuity equation (1.9) yields an equation for the perturbation pressure:

$$\nabla^2 p = -2U' \frac{\partial v}{\partial x}. \quad (1.10)$$

This equation may be used with equation (1.7) to eliminate p , resulting in an equation for the normal velocity, v . To do this, consider the ∇^2 of (1.7), with special care when applying the laplacian operator to the convective term $U \frac{\partial v}{\partial x}$.

$$\begin{aligned} \nabla \cdot \nabla \left(U \frac{\partial v}{\partial x} \right) &= \nabla \cdot \left(U \frac{\partial^2 v}{\partial x^2}, U' \frac{\partial v}{\partial x} + U \frac{\partial^2 v}{\partial x \partial y}, U \frac{\partial^2 v}{\partial x \partial z} \right) = \\ U \frac{\partial^3 v}{\partial x^3} + U'' \frac{\partial v}{\partial x} + U' \frac{\partial^2 v}{\partial x \partial y} + U \frac{\partial^3 v}{\partial x \partial y^2} + U' \frac{\partial^2 v}{\partial x \partial y} + U \frac{\partial^3 v}{\partial x \partial z^2} &= U \frac{\partial}{\partial x} \nabla^2 v + U'' \frac{\partial v}{\partial x} + 2U' \frac{\partial^2 v}{\partial x \partial y} \end{aligned} \quad (1.11)$$

The final equations is

$$\left[\left(\frac{\partial}{\partial t} + U \frac{\partial}{\partial x} \right) \nabla^2 - U'' \frac{\partial}{\partial x} - \frac{1}{\text{Re}} \nabla^4 \right] v = 0. \quad (1.12)$$

To describe the complete three-dimensional flow field, a second equation is needed. This is most conveniently the equation for the normal vorticity,

$$\eta = \frac{\partial u}{\partial z} - \frac{\partial w}{\partial x} \quad (1.13)$$

where η satisfies

$$\left[\frac{\partial}{\partial t} + U \frac{\partial}{\partial x} - \frac{1}{\text{Re}} \nabla^2 \right] \eta = -U' \frac{\partial v}{\partial z}. \quad (1.14)$$

This pair of equations with the boundary conditions

$$v = v' = \eta = 0 \quad \text{at a solid wall and in the far field} \quad (1.15)$$

and the initial conditions

$$\begin{aligned} v(x, y, z, t = 0) &= v_0(x, y, z) \\ \eta(x, y, z, t = 0) &= \eta_0(x, y, z) \end{aligned} \quad (1.16)$$

provides a complete description of the evolution of an arbitrary disturbance in both space and time. The second boundary condition for the velocity $v' = 0$ is derived directly from the continuity equation (1.9), noting that $\frac{\partial u}{\partial x} + \frac{\partial w}{\partial z} = 0$ at the wall.

1.2.3 Normal-mode assumption

Let us look for wavelike solutions of the form

$$\begin{aligned} v(x, y, z, t) &= \tilde{v}(y) e^{i(\alpha x + \beta z - \omega t)} \\ \eta(x, y, z, t) &= \tilde{\eta}(y) e^{i(\alpha x + \beta z - \omega t)} \end{aligned} \quad (1.17)$$

where α and β denote the streamwise and spanwise wave numbers, respectively, and ω stands for the frequency.

Introducing this representation into (1.12) and (1.14), or equivalently taking the Fourier transform in the horizontal directions, results in the following pair of equations for \tilde{v} and $\tilde{\eta}$

$$\left[(-i\omega + i\alpha U)(\mathcal{D}^2 - k^2) - i\alpha U'' - \frac{1}{\text{Re}}(\mathcal{D}^2 - k^2)^2 \right] \tilde{v} = 0 \quad (1.18)$$

$$\left[(-i\omega + i\alpha U) - \frac{1}{\text{Re}}(\mathcal{D}^2 - k^2) \right] \tilde{\eta} = -i\beta U' \tilde{v} \quad (1.19)$$

with the boundary conditions $\tilde{v} = \mathcal{D}\tilde{v} = \tilde{\eta} = 0$ at solid walls and in the free stream and $\mathcal{D} = \frac{\partial}{\partial y}$.

The equation for the normal velocity (1.18) is the classical Orr-Sommerfeld equation and the equation for the normal vorticity (1.19) is known as the Squire equation.

Although there is no general restriction to real or complex wave numbers or frequencies, we will mainly consider the temporal problem, where the spatial wave numbers α and β are assumed real, indicating waves infinitely extended in x and z . The frequency ω , or alternatively $c = \omega/\alpha$, appears as the eigenvalue in the Orr-Sommerfeld equation, and together with the associated eigenfunctions \tilde{v} is generally complex. The imaginary part of ω will indicate whether a specific wave is stable or not: unstable waves are characterized by positive imaginary part.

Alternatively, the spatial framework could be adopted. In this case, the spanwise wavenumber β and the frequency ω are real, while the complex streamwise wavenumber α indicates growth or decay in space.

1.2.4 Vector Modes

In the previous section we looked at the individual linear stability equations for parallel shear flows. In this section we will consider them as one system, which will result in more compact notation and easier algebraic manipulations when general results are derived.

We will start by introducing the vector quantity

$$\begin{pmatrix} \tilde{v} \\ \tilde{\eta} \end{pmatrix} \quad (1.20)$$

which allows us to write the Orr-Sommerfeld and Squire equations (1.18) and (1.19) in matrix form as

$$-i\omega \begin{pmatrix} k^2 - \mathcal{D}^2 & 0 \\ 0 & 1 \end{pmatrix} \begin{pmatrix} \tilde{v} \\ \tilde{\eta} \end{pmatrix} + \begin{pmatrix} \mathcal{L}_{OS} & 0 \\ i\beta U' & \mathcal{L}_{SQ} \end{pmatrix} \begin{pmatrix} \tilde{v} \\ \tilde{\eta} \end{pmatrix} = 0 \quad (1.21)$$

where

$$\begin{aligned} \mathcal{L}_{OS} &= i\alpha U(k^2 - \mathcal{D}^2) + i\alpha U'' + \frac{1}{\text{Re}}(k^2 - \mathcal{D}^2)^2 \\ \mathcal{L}_{SQ} &= i\alpha U + \frac{1}{\text{Re}}(k^2 - \mathcal{D}^2). \end{aligned} \quad (1.22)$$

The solution to this system, including boundary conditions, gives the eigenmodes discussed earlier. The off-diagonal coupling term, $i\beta U'$, in the matrix implies that the Squire equation is driven by solutions to the Orr-Sommerfeld equation, unless \tilde{v} or β is zero.

The eigenfunctions of the complete system can be divided into the two families of Orr-Sommerfeld and Squire modes previously defined. In the vector formulation they take the form

$$\begin{pmatrix} \tilde{v} \\ \tilde{\eta}^p \end{pmatrix} \quad \text{OS modes} \quad \begin{pmatrix} 0 \\ \tilde{\eta} \end{pmatrix} \quad \text{SQ modes.} \quad (1.23)$$

We like to emphasize that they are formally all eigenfunctions of the same system. It is only due to the zero off-diagonal term that they can be separated into two distinct families.

We now introduce a more compact notation. This is most easily accomplished by defining the vector

$$\tilde{\mathbf{q}} = \begin{pmatrix} \tilde{v} \\ \tilde{\eta} \end{pmatrix}. \quad (1.24)$$

The eigenvalue problem (1.21) now becomes

$$\mathbf{L}\tilde{\mathbf{q}} = i\omega\mathbf{M}\tilde{\mathbf{q}} \quad \text{or} \quad \mathbf{L}_1\tilde{\mathbf{q}} \equiv \mathbf{M}^{-1}\mathbf{L}\tilde{\mathbf{q}} = i\omega\tilde{\mathbf{q}} \quad (1.25)$$

where

$$\mathbf{M} = \begin{pmatrix} k^2 - \mathcal{D}^2 & 0 \\ 0 & 1 \end{pmatrix} \quad (1.26)$$

$$\mathbf{L} = \begin{pmatrix} \mathcal{L}_{OS} & 0 \\ i\beta U' & \mathcal{L}_{SQ} \end{pmatrix} \quad (1.27)$$

with \mathbf{M} as a positive definite operator.

1.3 Energy equation

Let us consider the kinetic energy of the perturbation $u_i u_i$. The analysis of this quantity provides interesting useful insight over the instability mechanisms and a justification for the linear analysis presented above. Without any initial assumption, an equation for the evolution of the perturbation energy can be derived upon scalar multiplication of the Navier-Stokes equations in perturbation form (1.5) with u_i . Using the fact that the flow is divergence free, we find that

$$\begin{aligned} u_i \frac{\partial u_i}{\partial t} &= -u_i u_j \frac{\partial U_i}{\partial x_j} - \frac{1}{\text{Re}} \frac{\partial u_i}{\partial x_j} \frac{\partial u_i}{\partial x_j} \\ &+ \frac{\partial}{\partial x_j} \left[-\frac{1}{2} u_i u_i U_j - \frac{1}{2} u_i u_i u_j \right. \\ &\quad \left. - u_i p \delta_{ij} + \frac{1}{\text{Re}} u_i \frac{\partial u_i}{\partial x_j} \right] \end{aligned} \quad (1.28)$$

Integrating the equation over the volume V , assuming that the disturbance is localized or spatially periodic, and using Gauss' theorem, we find the Reynolds-Orr equation

$$\frac{dE_V}{dt} = - \int_V u_i u_j \frac{\partial U_i}{\partial x_j} dV - \frac{1}{\text{Re}} \int_V \frac{\partial u_i}{\partial x_j} \frac{\partial u_i}{\partial x_j} dV. \quad (1.29)$$

In the expression above,

$$E_V = \frac{1}{2} \int_V u_i u_i dV.$$

All the terms that can be written as a divergence vanish when integrated over the volume V . They represent energy fluxes and give no net contribution to the energy balance: the terms indicate transport of kinetic energy by the mean flow, by the perturbations and by the work of the pressure and viscous forces respectively. In particular, it is important to realize that the nonlinear terms have dropped out. Due to the multiplication by u_i linear terms in (1.5) result in quadratic terms in (1.28); a nonlinear term in (1.5) thus corresponds to a cubic term in (1.28). The two remaining terms on the right-hand side of (1.29) represent the exchange of energy with the base flow and energy dissipation due to viscous effects, respectively.

The Reynolds-Orr equation (1.29) can be used to draw an important conclusion about the nature of growth mechanisms possible for disturbances on base flows that are solutions to the Navier-Stokes equations.

From (1.29) we observe that the instantaneous growth rate, $\frac{1}{E_V} \frac{dE_V}{dt}$, is independent of the disturbance amplitude. In other words, the growth rate of a finite-amplitude disturbance can, at each instant of its evolution, be found from an infinitesimal disturbance with an identical shape. Thus, the instantaneous growth rate of a finite-amplitude disturbance is given by mechanisms that are present in the linearized equations, and the total growth of a finite-amplitude disturbance can be regarded as a sum of growth rates associated with the linear mechanisms. This is a consequence of the conservative nature of the nonlinear terms in the Navier-Stokes equations.

This argument about the need for a linear energy source assumes that the total disturbance energy is based on deviations from a laminar base flow (U_i) that satisfies the Navier-Stokes equations. Alternatively, it is possible and common to measure the disturbance energy based on a mean flow modified by the disturbances, as, e.g., in the Reynolds averaging procedure frequently used in turbulence research. However, one of the advantages of using the decomposition leading to the nonlinear disturbance equation (1.5), is that in transition research one is frequently interested in measuring the departure of the disturbed flow from the initial laminar state.

Chapter 2

Inviscid results

2.1 Rayleigh equation

Following the historical evolution of the research in this field, we will consider the inviscid theory first. The effect of viscosity is therefore neglected and it is assumed that $\text{Re} \rightarrow \infty$. Let us consider two-dimensional perturbation, described by the Orr-Sommerfeld equation (1.18). In the limit above, the equation reduces to

$$\left[\left(\frac{\partial}{\partial t} + U \frac{\partial}{\partial x} \right) \nabla^2 - U'' \frac{\partial}{\partial x} \right] v = 0, \quad (2.1)$$

with boundary condition $v = 0$ on a solid wall. In the absence of viscosity, only the impermeability condition is imposed since zero tangential velocity is enforced by the requirement of finite viscous stress at the wall. This equation was derived by Lord Rayleigh equation in 1880. It is obtained directly from the linearized Navier-Stokes equation (1.6)-(1.8) following the same steps adopted in section 1.2 to derive the Orr-sommerfeld equation.

Assuming wavelike solutions and introducing the phase speed $c = \omega/\alpha$, the Rayleigh equation can be written as

$$\left[\mathcal{D}^2 - \alpha^2 - \frac{U''}{U - c} \right] \tilde{v} = 0, \quad (2.2)$$

with $\tilde{v} = 0$ at solid boundaries. Two remarks can be immediately reported.

Remark I: the Rayleigh equation (2.2) has real coefficients. As a consequence, its eigenvalues can be either real or complex conjugate pairs. These correspond to neutral waves and to a pair of stable/unstable waves with the same phase speed c_r . Therefore purely damped modes cannot be found.

Remark II: the Rayleigh equation (2.2) has a regular singular point at $y_c : U(y_c) = c$. The solution can be obtained in the vicinity of this point via a Frobenius expansion, see [7]. The location $y = y_c$ is denoted as critical layer. Here, we would like to note that from a physical point of view, the presence of a singularity indicates that viscous effects are important in this region. There are thus two layers where viscosity should be considered even in the limit $\text{Re} \rightarrow \infty$.

1. At the boundary where only one boundary condition can be satisfied in the inviscid limit, in close analogy to the derivation of the boundary layer equations by Prandtl.
2. At the critical layer where the stability problem is singular.

In the literature, one can find several asymptotic studies on the solution of the stability of a parallel shear flow in the limit of vanishing viscosity. The thickness of these two layers is found to be of the order $\mathcal{O}(\alpha \text{Re}^{1/2})$ at the wall and $\mathcal{O}(\alpha \text{Re}^{1/3})$ at the critical layer.

Starting from the Rayleigh equation (2.2), a few general results can be derived without specifying a particular mean velocity profile. Two of these results will be presented here: Rayleigh's inflection point criterion and Fjørtoft's criterion.

2.1.1 Rayleigh's inflection point criterion

Rayleigh's inflection point criterion relates the existence of an unstable mode to the occurrence of an inflection point in the mean velocity profile. We will assume a bounded flow domain with $y \in [-1, 1]$.

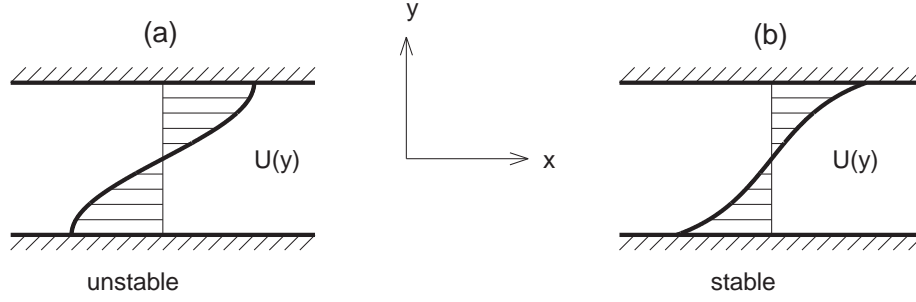


Figure 2.1: Demonstration of Fjörtoft's criterion as a necessary condition for instability in inviscid flow. (a) unstable according to Fjörtoft, (b) stable according to Fjörtoft.

Theorem 2.1.1 (Rayleigh's inflection point criterion). *If there exist perturbations with $c_i > 0$, then $U''(y)$ must vanish for some $y_s \in [-1, 1]$.*

The proof of this theorem is given by multiplying the Rayleigh equation (2.2) by the complex conjugate of the normal velocity, \tilde{v}^* , and integrating in y from -1 to 1 . After integrating by parts we obtain the equation

$$\int_{-1}^1 |\mathcal{D}\tilde{v}|^2 + k^2|\tilde{v}|^2 dy + \int_{-1}^1 \frac{U''}{U-c} |\tilde{v}|^2 dy = 0. \quad (2.3)$$

The first integral is real and positive definite, and the second integral is in general complex-valued. Taking the imaginary part of the above expression yields

$$\text{Im} \left\{ \int_{-1}^1 \frac{U''}{U-c} |\tilde{v}|^2 dy \right\} = \int_{-1}^1 \frac{U'' c_i |\tilde{v}|^2}{|U-c|^2} dy = 0. \quad (2.4)$$

Both $|\tilde{v}|^2$ and $|U-c|^2$ are nonnegative and c_i has been assumed positive. It follows that U'' has to change sign to render the integral zero. The theorem follows immediately from this conclusion. Rayleigh's inflection point criterion only gives a necessary condition for instability.

A physical interpretation can be given considering vortex filaments...

2.1.2 Fjörtoft's criterion

An extension of the inflection point criterion (2.4) due to Fjörtoft provides an improved necessary condition for instability.

Theorem 2.1.2 (Fjörtoft's criterion). *Given a monotonic mean velocity profile $U(y)$, a necessary condition for instability is that $U''(U-U_s) < 0$ for $y \in [-1, 1]$, with $U_s = U(y_s)$ as the mean velocity at the inflection point, i.e., $U''(y_s) = 0$.*

This means that the inflection point has to be a maximum (rather than a minimum) of the spanwise mean vorticity. Fjörtoft's criterion can be derived by considering the real part of equation (2.3). We get

$$\int_{-1}^1 \frac{U''(U-c_r)}{|U-c|^2} |\tilde{v}|^2 dy = - \int_{-1}^1 |\mathcal{D}\tilde{v}|^2 + k^2|\tilde{v}|^2 dy. \quad (2.5)$$

Next, we add the expression

$$(c_r - U_s) \int_{-1}^1 \frac{U''}{|U-c|^2} |\tilde{v}|^2 dy \quad (2.6)$$

to the left side of the equation. This expression is identically zero due to the inflection point criterion (2.4). We then obtain

$$\int_{-1}^1 \frac{U''(U-U_s)}{|U-c|^2} |\tilde{v}|^2 dy = - \int_{-1}^1 |\mathcal{D}\tilde{v}|^2 + k^2|\tilde{v}|^2 dy. \quad (2.7)$$

For the integral on the left to be negative, we have to require the expression $U''(U - U_s)$ to be negative somewhere in the flow field. This concludes the proof of Fjørtoft's theorem.

Figure 2.1 demonstrates Rayleigh's and Fjørtoft's criteria as necessary conditions for instability of inviscid fluid flow. Both mean velocity profiles show an inflection point in the center of the channel, and thus they satisfy Rayleigh's necessary condition for an inviscid instability. However, only the velocity profile on the left fulfills Fjørtoft's criterion in addition to Rayleigh's. The mean velocity profile on the right has a minimum (rather than a maximum) of the spanwise mean vorticity and therefore does not satisfy Fjørtoft's criterion.

2.2 Inviscid algebraic instability

In this section we show that significant growth of the perturbation amplitude can be observed also for velocity profiles without an inflection point. It cannot be the exponential growth of a linearly unstable wave but rather the algebraic growth of perturbations with a specific initial shape. For the derivation the work of Ellingsen and Palm (1975) is followed [1]. These authors showed that disturbances independent of the streamwise coordinate may lead to instability of the linear flow $U = Cy$, even though the basic velocity profile does not possess an inflection point.

Let us consider the Rayleigh equation (2.1) for streamwise independent velocity v

$$\frac{\partial}{\partial t} \nabla^2 v = 0,$$

which implies that v is independent of time. Wall-normal velocity disturbances are therefore just convected by the mean flow U .

When considering the evolution of the disturbance streamwise velocity component, the following linearized equation is obtained (again $\frac{\partial}{\partial x} = 0$)

$$\frac{Du}{Dt} = 0 \Rightarrow \frac{\partial u}{\partial t} + v \frac{\partial U}{\partial y} = 0,$$

which can be integrated easily for the base flow considered here to yield

$$\frac{\partial u}{\partial t} = -vC \rightarrow u = u(0) - vkt. \quad (2.8)$$

The streamwise velocity perturbation is therefore linearly growing in time. The second term accounts for the integrated effect of the normal velocity, the so-called lift-up effect, see [4]. This term represents the generation of horizontal velocity perturbations by the lifting-up of fluid elements in the presence of the mean shear.

2.3 Kelvin-Helmholtz instability

We consider now the instability at the interface between two horizontal parallel streams of different velocity U_1 and U_2 , assumed constant in the cross-stream direction y , and different densities ρ_1 and ρ_2 . The case of heavier fluid at the bottom can be used to model instabilities developing in clouds. Note that the name Kelvin-Helmholtz instability is used to denote also instabilities in flows where the velocity is varying over a finite length as in the case mixing layers and jets.

We will apply the Rayleigh equation (2.2) to the two layers, where $U'' = 0$ and the subscript 1, 2 denote the top and bottom stream respectively,

$$[(U - c)(\mathcal{D}^2 - \alpha^2)] v_{1,2} = 0, \quad (2.9)$$

with boundary conditions

$$\tilde{v}_1 \rightarrow 0 \quad \text{as } y \rightarrow \infty; \quad \tilde{v}_2 \rightarrow 0 \quad \text{as } y \rightarrow -\infty. \quad (2.10)$$

Conditions at the interface between the two streams are needed to close the problem. They are a kinematic condition, requiring continuity of the interface surface, and a dynamic condition, requiring continuity of the pressure. Let us define the interface surface as

$$y = y_0 + \zeta(x, t),$$

where y_0 is the undisturbed reference location and ζ a small deviation. If we require that the interface is moving with the local velocity

$$v = \frac{Dy}{Dt} = \left[\frac{\partial}{\partial t} + (U + u) \frac{\partial}{\partial x} \right] \zeta.$$

Assuming wavelike solutions $\zeta = \tilde{\zeta} \exp i(\alpha x - \omega t)$ and linearizing for small deformations, the following relation, valid in 1 and 2 is obtained

$$\tilde{v}_{1,2} = (-i\omega + iU_{1,2}\alpha) \tilde{\zeta}. \quad (2.11)$$

Let us now consider the dynamic condition. An equation for the pressure can be derived from the inviscid linearized Navier-Stokes equations with g the gravitational acceleration acting in the negative y -direction

$$\frac{\partial u}{\partial t} + U \frac{\partial u}{\partial x} + vU' = -\frac{1}{\rho} \frac{\partial p}{\partial x} \quad (2.12)$$

$$\frac{\partial v}{\partial t} + U \frac{\partial v}{\partial x} = -\frac{1}{\rho} \frac{\partial p}{\partial y} - g \quad (2.13)$$

$$\frac{\partial u}{\partial x} + \frac{\partial v}{\partial y} = 0. \quad (2.14)$$

Taking the x-derivative of equation (2.12)

$$\frac{\partial}{\partial t} \frac{\partial u}{\partial x} + U \frac{\partial^2 u}{\partial x^2} + \frac{\partial v}{\partial x} U' = -\frac{1}{\rho} \frac{\partial^2 p}{\partial x^2},$$

and using the continuity equation (2.14), the following equation relating v and p is obtained

$$-\frac{\partial}{\partial t} \frac{\partial v}{\partial y} - U \frac{\partial^2 v}{\partial x \partial y} + \frac{\partial v}{\partial x} U' = -\frac{1}{\rho} \frac{\partial^2 p}{\partial x^2}.$$

Applying the Fourier transform and solving for \tilde{p} ,

$$\tilde{p} = \frac{i\rho}{\alpha} [(c - U)\mathcal{D}\tilde{v} + U'\tilde{v}] + F(y), \quad (2.15)$$

where $F(y) = \tilde{p}_0 - \rho gy$ accounts for the hydrostatic pressure, effect of gravity. Thus, the continuity of the pressure at the interface can be expressed as

$$\rho_1 \left[\frac{i}{\alpha} (U_1 - c) \mathcal{D}\tilde{v}_1 + g\tilde{\zeta} \right] = \rho_2 \left[\frac{i}{\alpha} (U_2 - c) \mathcal{D}\tilde{v}_2 + g\tilde{\zeta} \right], \quad (2.16)$$

where we have used ζ to define the interface displacement and the fact that $U' = 0$.

We can now solve equations (2.9) with boundary conditions (2.10), (2.11) and (2.16). Evaluating the disturbance velocity for the two horizontal streams from

$$(\mathcal{D}^2 - \alpha^2) \tilde{v}_{1,2} = 0,$$

the following solutions are obtained

$$\tilde{v}_{1,2} = A_{1,2} e^{-\alpha y} + B_{1,2} e^{\alpha y};$$

by enforcing the boundary conditions (2.10), the solutions reduce to

$$\tilde{v}_1 = A_1 e^{-\alpha y}; \quad \tilde{v}_2 = B_2 e^{\alpha y}. \quad (2.17)$$

Let us first use the kinematic condition to express $\tilde{v} = \tilde{v}(\tilde{\zeta})$, A_1 and B_2 . In the limit of linear perturbations and deformations, the surface is assumed to be at $y = y_0 = 0$ and the displacement $\tilde{\zeta}$ can be written as

$$\tilde{\zeta} = \frac{\tilde{v}_1}{i\alpha(U_1 - c)} \Big|_0 = \frac{\tilde{v}_2}{i\alpha(U_2 - c)} \Big|_0. \quad (2.18)$$

Combining equations (2.17) and (2.18), the following values for the integration constants are obtained

$$A_1 = i\alpha(U_1 - c) \quad (2.19)$$

$$B_2 = i\alpha(U_2 - c). \quad (2.20)$$

The dynamic condition can be finally used to express the dispersion relation for the Kelvin-Helmholtz instability,

$$\rho_1 \left[\frac{i}{\alpha} (U_1 - c)(-\alpha i \alpha)(U_1 - c)\tilde{\zeta} + g\tilde{\zeta} \right] = \rho_2 \left[\frac{i}{\alpha} (U_2 - c)(\alpha i \alpha)(U_2 - c)\tilde{\zeta} + g\tilde{\zeta} \right], \quad (2.21)$$

$$\alpha \rho_2 (U_2 - c)^2 + \alpha \rho_1 (U_1 - c)^2 = g(\rho_2 - \rho_1), \quad (2.22)$$

and finally

$$c = \frac{\rho_2 U_2 - \rho_1 U_1}{\rho_2 + \rho_1} \pm \sqrt{\frac{g}{\alpha} \frac{\rho_2 - \rho_1}{\rho_2 + \rho_1} - \rho_1 \rho_2 \left(\frac{U_1 - U_2}{\rho_2 + \rho_1} \right)^2}. \quad (2.23)$$

As noted above, either real or complex conjugate solutions are possible. The flow is therefore unstable when the argument of the square root is negative,

$$c_i > 0 \quad \text{if} \quad g(\rho_2^2 - \rho_1^2) < \alpha \rho_1 \rho_2 (U_1 - U_2)^2.$$

From the above, it can be seen that gravity, through the density difference, has a stabilizing effect. (This is true if the bottom layer is heavier, otherwise the flow is always unstable). Further, if there is a velocity difference, $U_1 \neq U_2$, it is possible to find a wave with large enough α to be unstable. Thus, the flow is always unstable to short enough waves. Note that viscosity is neglected here.

2.3.1 Instability of a vortex sheet

Let us consider two streams of homogeneous fluid, $\rho_1 = \rho_2$. The dispersion relation reduces to

$$c = \frac{1}{2}(U_1 + U_2) \pm \frac{i}{2}(U_1 - U_2) = \bar{U} \pm i \frac{\Delta U}{2}.$$

The growth rate

$$\omega = \alpha \bar{U} \pm i \alpha \frac{\Delta U}{2}$$

is then proportional to the wavenumber α . Note that there is no intrinsic length scale in the problem, and no cutoff wavenumber for the instability is found.

Physical interpretation, vortex filaments, Batchelor 1967

2.3.2 The piecewise mixing layer

To represent a more realistic velocity profile and introduce a characteristic length, denoted vorticity thickness, where the velocity variation occurs, we consider the stability of a mixing layer where the velocity profile has been approximated by straight lines, as shown in Figure 2.2. The velocity profile is given as

$$U(y) = \begin{cases} 1 & \text{for } y > 1 \\ y & \text{for } -1 \leq y \leq 1 \\ -1 & \text{for } y < -1. \end{cases} \quad (2.24)$$

We will denote the upper part of the velocity profile ($y > 1$) region I, the middle part ($-1 \leq y \leq 1$) region II or vorticity layer since the base flow is not zero here, and the lower part ($y < -1$) region III (see Figure 2.2). Because the second derivative term for the mean velocity profile vanishes, the Rayleigh equation (2.2) reduces to the simpler equation

$$(\mathcal{D}^2 - \alpha^2)\tilde{v} = 0 \quad (2.25)$$

which has to be solved in all regions subject to the boundary conditions

$$\tilde{v} \rightarrow 0 \quad \text{as } y \rightarrow \pm\infty \quad (2.26)$$

and the appropriate matching conditions.

The solution of (2.25) satisfying the boundary condition in regions I to III is found to be

$$\tilde{v}_I = A \exp(-\alpha y) \quad \text{for } y > 1 \quad (2.27)$$

$$\tilde{v}_{II} = B \exp(-\alpha y) + C \exp(\alpha y) \quad \text{for } -1 \leq y \leq 1 \quad (2.28)$$

$$\tilde{v}_{III} = D \exp(\alpha y) \quad \text{for } y < -1. \quad (2.29)$$

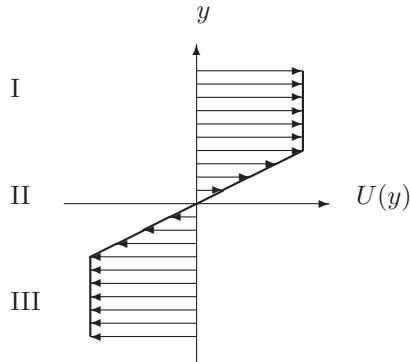


Figure 2.2: Sketch of the piecewise linear mixing layer.

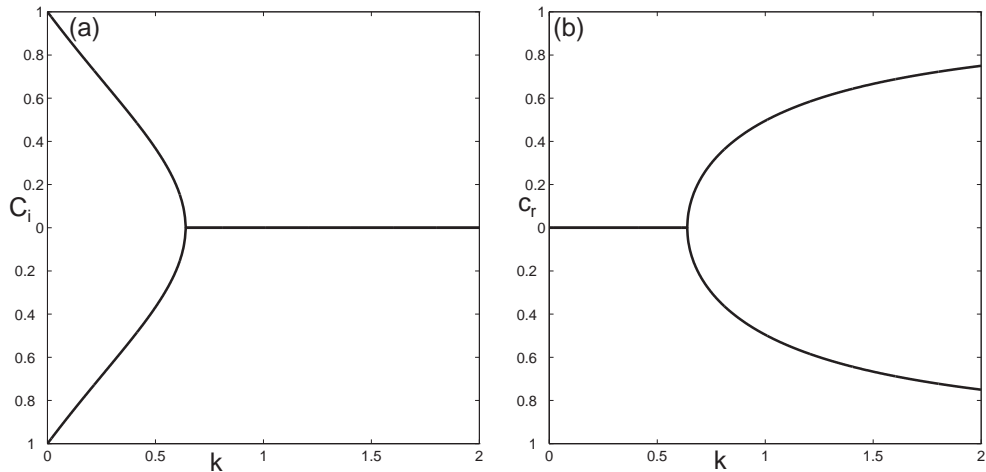


Figure 2.3: Eigenvalues for the piecewise linear mixing layer. (a) Imaginary part of the eigenvalue (growth rate) as a function of wave number. (b) Real part of the eigenvalue (phase speed) as a function of wave number.

The constants A, B, C , and D have to be found by enforcing the matching conditions across the points $y = \pm 1$. From matching the velocity and pressure across the point $y = 1$, we get

$$2C\alpha(1 - c) \exp(\alpha) = B \exp(-\alpha) + C \exp(\alpha) \quad (2.30)$$

and from matching across the point $y = -1$, we obtain

$$2B\alpha(1 + c) \exp(\alpha) = B \exp(\alpha) + C \exp(-\alpha). \quad (2.31)$$

Both unknown coefficients B and C can be eliminated from these equations, leaving us with a condition on the eigenvalue c of the form

$$c = \pm \sqrt{\left(1 - \frac{1}{2\alpha}\right)^2 - \left(\frac{1}{4\alpha^2}\right) \exp(-4\alpha)}. \quad (2.32)$$

A plot of the dispersion relation is given in Figure 2.3. For the range of wave numbers $0 \leq \alpha \leq 0.6392$ the expression under the square root is negative, resulting in purely imaginary eigenvalues c . For wave numbers larger than $\alpha = 0.6392$ the eigenvalues are real, and all disturbances are neutral. The eigenfunctions are displayed in Figure 2.4. As the wave number goes to zero, the wavelength associated with the disturbances is much larger than the length scale associated with the mean velocity profile. The limit of small wave numbers is thus equivalent to the limit of a zero thickness of region II. In this case we recover the stability results for the Kelvin-Helmholtz instability considered above with $U_1 = 1$ and $U_2 = -1$, namely,

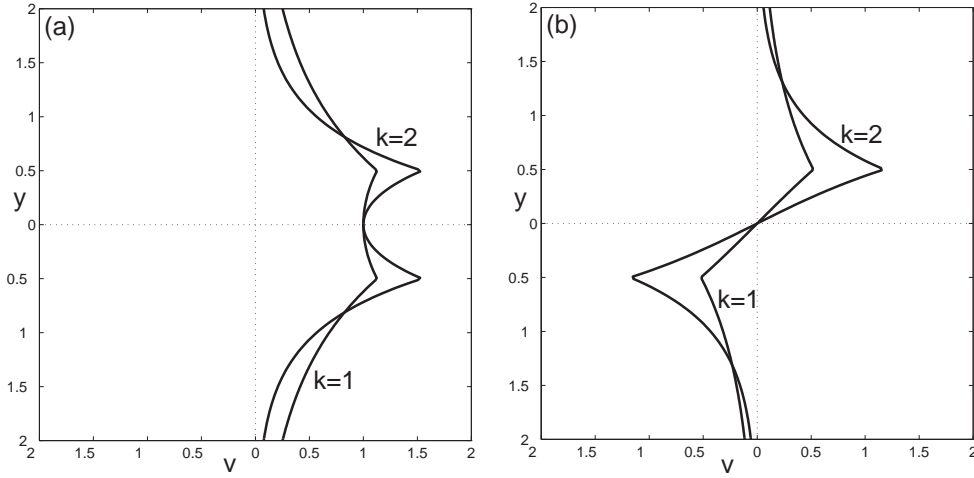


Figure 2.4: Eigenfunctions for the piecewise linear mixing layer for $k = 1$ and $k = 2$. (a) Symmetric eigenfunction; (b) antisymmetric eigenfunction.

$$\lim_{\alpha \rightarrow 0} c^2(\alpha) = \lim_{\alpha \rightarrow 0} \frac{4\alpha^2 - 4\alpha + 1 - \exp(-4\alpha)}{4k^2} = -1$$

or

$$c = \pm i. \tag{2.33}$$

Thus the eigenvalues for this case are independent of the wave number. Thus, wavelike perturbations on an unbounded vortex sheet in an inviscid fluid do not show any dispersion, i.e., all wave components travel at the same (zero) speed. Conversely, in the case of large α , the waves are mainly living in the vorticity layer and see a linear velocity distribution. They are therefore stable. A cutoff wavenumber is thus introduced in our system, not by viscosity, but by the characteristic length scale of the problem, the vorticity thickness.

Chapter 3

Viscous stability

In this chapter we will present solutions of the Orr-Sommerfeld and Squire equations derived in chapter 1,

$$\left[(-i\omega + i\alpha U)(\mathcal{D}^2 - k^2) - i\alpha U'' - \frac{1}{\text{Re}}(\mathcal{D}^2 - k^2)^2 \right] \tilde{v} = 0 \quad (3.1)$$

$$\left[(-i\omega + i\alpha U) - \frac{1}{\text{Re}}(\mathcal{D}^2 - k^2) \right] \tilde{\eta} = -i\beta U' \tilde{v} \quad (3.2)$$

with the boundary conditions $\tilde{v} = \mathcal{D}\tilde{v} = \tilde{\eta} = 0$ at solid walls and in the free stream. Note that both equations are necessary to describe three-dimensional perturbations, i.e. $\alpha \neq 0$, $\beta \neq 0$ and that viscous effects are now taken into account. It is also important to mention that inviscid theory has proven to be good at predicting the instability of free shear flows (jets, wakes, mixing layers) where the mean velocity profile possess an inflection point. These flows usually become unstable at relatively low Reynolds numbers, e.g. $\text{Re} \approx 40$ for jets, and inviscid analysis at the Reynolds number of typical interest is enough. However, wall-bounded shear flows (channel flows and boundary layers) do not present an inflection point and viscous analysis is needed to capture correctly the flow behavior, as we show below.

3.1 Squire's Transformation and Squire's Theorem

3.1.1 Relation between the two-dimensional and three-dimensional solutions

Instead of considering the complex frequency ω as the eigenvalue one often uses the complex phase speed c , where

$$\omega = \alpha c \quad (3.3)$$

which results in the following slightly different version of the Orr-Sommerfeld equation (1.18)

$$(U - c)(\mathcal{D}^2 - k^2)\tilde{v} - U''\tilde{v} - \frac{1}{i\alpha \text{Re}}(\mathcal{D}^2 - k^2)^2\tilde{v} = 0. \quad (3.4)$$

Squire's transformation is found by comparing this equation to the two-dimensional Orr-Sommerfeld equation, i.e., the Orr-Sommerfeld equation with $\beta = 0$, given as

$$(U - c)(\mathcal{D}^2 - \alpha_{2D}^2)\tilde{v} - U''\tilde{v} - \frac{1}{i\alpha_{2D} \text{Re}_{2D}}(\mathcal{D}^2 - \alpha_{2D}^2)^2\tilde{v} = 0. \quad (3.5)$$

Comparing these two equations, it is evident that they have identical solutions if the following relations hold

$$\begin{aligned} \alpha_{2D} &= k = \sqrt{\alpha^2 + \beta^2} \\ \alpha_{2D} \text{Re}_{2D} &= \alpha \text{Re} \end{aligned} \quad (3.6)$$

from which it follows that

$$\text{Re}_{2D} = \text{Re} \frac{\alpha}{k} < \text{Re}. \quad (3.7)$$

This states that to each three-dimensional Orr-Sommerfeld mode corresponds a two-dimensional Orr-Sommerfeld mode at a *lower* Reynolds number.

3.1.2 Damped Squire modes

Before we state Squire's theorem, we will prove the following.

Theorem 3.1.1 (Damped Squire modes). *The solutions to the Squire equation are always damped, i.e., $c_i < 0$ for all α , β , and Re .*

The theorem is proved by first multiplying the homogeneous Squire equation (1.19) by $\tilde{\eta}^*$, the complex conjugate of the normal vorticity, and integrating in the y -direction across the fluid domain, which for simplicity we take from -1 to 1 . We find

$$c \int_{-1}^1 \tilde{\eta}^* \tilde{\eta} dy = \int_{-1}^1 U \tilde{\eta}^* \tilde{\eta} dy - \frac{i}{\alpha Re} \int_{-1}^1 \tilde{\eta}^* (-\mathcal{D}^2 + k^2) \tilde{\eta} dy. \quad (3.8)$$

Taking the imaginary part of equation (3.8) and integrating by parts, we obtain

$$\begin{aligned} c_i \int_{-1}^1 |\tilde{\eta}|^2 dy &= -\frac{1}{\alpha Re} \int_{-1}^1 (-\tilde{\eta}^* \mathcal{D}^2 \tilde{\eta} + k^2 |\tilde{\eta}|^2) dy \\ &= -\frac{1}{\alpha Re} \int_{-1}^1 |\mathcal{D} \tilde{\eta}|^2 + k^2 |\tilde{\eta}|^2 dy < 0 \end{aligned} \quad (3.9)$$

which concludes the proof.

3.1.3 Squire's theorem

Theorem 3.1.2 (Squire's theorem). *Given Re_L as the critical Reynolds number for the onset of linear instability for a given α, β , the Reynolds number Re_c below which no exponential instabilities exist for any wave numbers satisfies*

$$Re_c \equiv \min_{\alpha, \beta} Re_L(\alpha, \beta) = \min_{\alpha} Re_L(\alpha, 0). \quad (3.10)$$

Thus parallel shear flows first become unstable to two-dimensional wavelike perturbations at a value of the Reynolds number that is smaller than any value for which unstable three-dimensional perturbations exist.

The proof of this theorem follows directly from Squire's transformation: If a three-dimensional mode is unstable, a two-dimensional mode is unstable at a lower Reynolds number.

3.2 Spectra and eigenfunctions

3.2.1 Continuous spectrum

3.2.2 Neutral stability curves

3.2.3 The destabilising effect of viscosity

One may have noticed that velocity profiles without an inflection point, so stable in the inviscid limit, actually become unstable once viscosity is considered. In this section, we aim therefore at explaining the subtle effect of viscosity in the instability of wall-bounded shear flows.

Let us consider the Reynolds-Orr equation governing the evolution of the perturbation kinetic energy

$$\frac{dE}{dt} = -u_i u_j \frac{\partial U_i}{\partial x_j} - \frac{1}{Re} \frac{\partial u_i}{\partial x_j} \frac{\partial u_i}{\partial x_j}. \quad (3.11)$$

Assuming channel flow in the domain $y \in [-1, 1]$ and temporal waves, i.e. perturbations periodic in space and growing in time, one can perform spatial averaging of the equation (3.11) by integrating in x and z over one wavelength of the perturbation,

$$\frac{d}{dt} \int_{-1}^1 E dy = - \int_{-1}^1 \overline{uv} U' dy - \frac{1}{Re} \int_{-1}^1 \overline{\frac{\partial u_i}{\partial x_j} \frac{\partial u_i}{\partial x_j}} dy. \quad (3.12)$$

where the integral extend across the channel and the overline denotes spatial averaging. Note that we have used the fact that for a channel flow $U = U(y)$ and therefore only the contribution from the Reynolds stress \overline{uv} is left in the production term in equation (3.11).

At first sight viscosity has only the stabilising effect associated to dissipation. A closer look at the Reynolds stress, however, reveals the effect of viscosity. Having assumed wavelike solutions, the Reynolds stress can be re-written

$$\tau_{xy} = -\overline{uv} = -(\tilde{u}\tilde{v}^* + \tilde{u}^*\tilde{v})e^{2kc_it} = -\frac{1}{2}|\tilde{u}(y)||\tilde{v}(y)|\cos[\phi_u(y) - \phi_v(y)]e^{2kc_it} \quad (3.13)$$

where * denotes the complex conjugate transpose, the exponential behavior is given by

$$\exp(i\alpha(x - c_r t) + kc_it) \cdot \exp(-i\alpha(x - c_r t) + kc_it),$$

and the complex eigenfunction is re-expressed as $\tilde{u}(y) = |\tilde{u}(y)|\exp(i\phi_u(y))$. Recalling that inviscid waves are either unstable or neutral, for profiles with no inflection point $c_i = 0$ and \tilde{u} and \tilde{v} are therefore in quadrature, $[\phi_u(y) - \phi_v(y)] = \pm\pi/2$. For finite Reynolds numbers viscosity is changing this phase difference. This may lead to a positive production term. This positive production may be large enough to overcome the dissipation also introduced by viscosity. Thus, unstable waves can be found at intermediate Reynolds number: not too high so that the effect of viscosity is felt on the Reynolds stress and not too low where dissipation would prevail over production.

Bibliography

- [1] T. Ellingsen and E. Palm. Stability of linear flow. *Phys. Fluids*, 18:487–488, 1975.
- [2] Th. Herbert. On perturbation methods in nonlinear stability theory. *J. Fluid Mech.*, 126:167–186, 1983.
- [3] P. S. Klebanoff, K. D. Tidstrom, and L. M. Sargent. The three-dimensional nature of boundary layer instability. *J. Fluid Mech.*, 12:1–34, 1962.
- [4] M. T. Landahl. A note on an algebraic instability of inviscid parallel shear flows. *J. Fluid Mech.*, 98:243–251, 1980.
- [5] W. M. F. Orr. The stability or instability of the steady motions of a perfect liquid and of a viscous liquid. Part I: A perfect liquid. Part II: A viscous liquid. *Proc. R. Irish Acad. A*, 27:9–138, 1907.
- [6] H. Schlichting. Berechnung der anfachung kleiner störungen bei der plattenströmung. *ZAMM*, 13:171–174, 1933.
- [7] P. J. Schmid and D. S. Henningson. *Stability and Transition in Shear Flows*. Springer, New York, 2001.
- [8] G. B. Schubauer and H. K. Skramstad. Laminar boundary layer oscillations and the stability of laminar flow. *J. Aero. Sci.*, 14:69–78, 1947.
- [9] A. Sommerfeld. Ein beitrag zur hydrodynamischen erklärung der turbulenten flüssigkeitbewegungen. In *Atti. del 4. Congr. Internat. dei Mat. III, Roma*, pages 116–124, 1908.
- [10] W. Tollmien. Über die entstehung der turbulenz. *Nachr. Ges. Wiss. Göttingen 21-24*,, 1929. English translation NACA TM 609, 1931.